The effect of lung tumor cluster-derived extracellular vesicles on the integrity of a mono- and multi-layered vessel on a chip model

The challenging viscous finger patterning technique

N.A. van Loenen, dr.ir. K.M. Pondman, prof.dr.ir. S. Le Gac

University of Twente — Applied Microfluidics for BioEngineering Research — EEMCS — July 4, 2023

Abstract

Lung cancer is characterised by a high rate of mortality and metastasis. Lately, extracellular vesicles (EVs) have gained attention as key players in preparing the pre-metastatic niche (PMN) by promoting vascular leakage. Vessel-on-a-chip (VoC) models are efficient and involve human physiological components that give more insights in the mechanism of vascular leakage. Using viscous finger patterning (VFP), renowned as a simple and reproducible technique, cylindrical mono- and multilayered vessels can be created. Also the uprise of microfluidic devices allows the application of flow inside VoCs. With the ability to more and more accurately mimic a physically correct human blood vessel, research on effect of EVs could be conducted with higher reliability. In this study, an optimized VFP method was used for the patterning of both mono- and multi-layered VoCs. To study the effect of EVs, lung tumor clusters were prepared and the tumor-conditioned medium was filtered to only obtain the tumor-derived EVs (tdEVs). To test the permeability of the formed VoCs, the vessels were stimulated with either EVs or a positive control being TNF-α or negative control being plain medium for deterioration of integrity. After this experiment, immunostaining for tight junctions was conducted to analyse the integrity of the vessel barriers. This way, the possible promotion of vascular leakage by tdEVs could be indicated. As a pilot experiment, the VoCs were also subjected to a flow to analyse the cell alignment under these conditions. Although the outcomes of this research were inconclusive regarding the isolation and effect of EVs on VoCs, further research on EVs using more complex organ-on-a-chip models for different mechanisms underlying PMN formation could show great potential for the prevention and treatment of metastatic tumors.

Keywords: Extracellular vesicles (EVs), vessel-on-a-chip (VoC), viscous finger patterning (VFP), lung cancer, mono-layer, multi-layer, ZO-1, pre-metastatic niche (PMN), blood vessel integrity

1 Introduction

Even with the present-day developments of health and technology, cancer is still one of the leading causes of death in the world. Lung cancer, with over 10.000 deaths in the Netherlands every year, has the highest mortality rate of all cancers [1]. When diagnosed, in 50% of the cases metastasis has already occurred: the tumor has spread to other organs, making the disease almost untreatable [2].

To be able to diagnose patients earlier and treat lung cancer metastasis effectively, the underlying mechanism of tumor metastasis has to be researched. Over a century ago, it was already established that metastasis takes place organ-specifically [3]. Preferential sites for lung cancer-derived metastasis are the lung, brain and bone, because all are equipped with a microvasculature and bear other favorable characteristics [4]. Not only the primary tumor, but also the environment at the pre-metastatic site plays a role in the ability of the tumor to metastasize, giving rise to the 'seed and soil' hypothesis [3]. Primary tumors can somehow shape the micro-environment of distant organs, the soil, before metastatic colonization of circulating tumor cell (CTC), the seeds, see Figure 1. This supportive micro-environment is nowadays known as the pre-metastatic niche (PMN).

In recent research, the versatile role of extracellular vesicles (EVs) in preparation of PMN has become more recognised. First considered as 'garbage cans', EVs have now gained attention as key players in cell-cell communication [4, 5]. EVs are lipid bilayer membranous vesicles ranging from 50-1000 nm released by cells carrying bio-active cargo [6, 4].EVs is a broad term, including exosomes, microvesicles apoptotic bodies and migratory bodies. With their ability to transport components, EVs support cell-cell communication and are able to start many of the required steps of PMN formation.

The first step of establishment of PMN is vascular leakage. During this process, blood vessels lose their integrity causing increased permeability and allowing the entrance of tumor cells and macromolecules at the site of metastasis [6, 4]. Multiple studies have shown the role of EVs in vascular leakage by stressing the local endothelial cells and breaking down adhesion molecules [6]. Because of this important role of EVs in the formation of PMN, inhibiting the formation and secretion of EVs or manipulating their bio-active cargo could form effective means to preventing metastasis and treating metastatic tumors [4].

Thus for EVs to reach and form the PMN, the bloodstream is very important. To be able to test the influence of EVs on blood vessel integrity and find ways

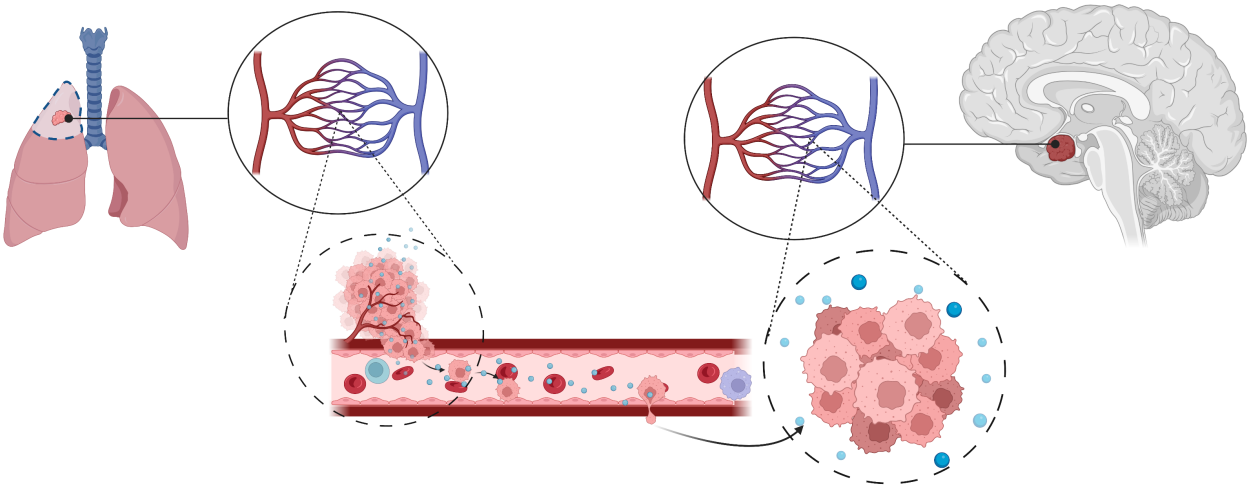

Figure 1: A schematic figure of the metastasis of circulating lung tumor clusters inside the brain. A lung CTC escapes inside the bloodstream (left) with the use of EVs (blue) and reaches the PMN inside brain tissue (right) due to vascular leakage. Created with BioRender.com.

to efficiently suppress metastasis [7], it is important to find and test models for blood vessels mimicking the in vivo vasculature, replicating the anatomical structure of blood vessels. Although *in vivo* animal tests are used as a standard method, they have a lot of limitations [8]. They have high experimental costs, limited throughput, ethical concerns, and show differences in genetic background, causing a lot of physiological differences in response to drugs and expression of diseases compared with humans [9]. Complex *in vitro* models like vessel-on-a-chip (VoC) models pose a solution since they involve procedures that use all human physiological components. However most of the commonly used techniques experience difficulties with upscaling, creating a consistent lumen and generating flow through [10].

To overcome challenges mentioned above, the technique of viscous finger patterning is more frequently used[11, 10, 12]. This microfluidic technique is based on the fact that when low viscosity fluid is inserted inside a higher viscosity fluid inside the microchannel, the less viscous fluid displaces the high viscosity fluid along the length of a microchannel, leaving behind a continuous cylindrical lumen in the middle of the microchannel [10]. This way, microfluidic devices containing blood vessel-like structures can be created by passive pumping due to a pressure difference between the inlet and the outlet [11]. There have been many successful attempts so far in the field of organ on a chip research, proving the potential of this facile and rapid technique [12]

Most VoCs used in research consist of only an endothelial layer. Although mono-layered VoC are useful for mimicking of unstable blood vessels, to create a physiological resemblance, a multi-layer must be established. Most capillaries consist of both an endothelial and a perivascular layer. The last one is very important, since it gives rise to the stability and integrity of the vessel barrier [11]. There have been several successful attempts of creating multi-layered VoCs [11]. However, to the best of our knowledge, only mono-layered VoCs have been used for research of EVs [13]. Also, during this research the main focus is isolation and characterisation of EVs, but not the effect on the VoCs used [14, 15, 16].

Final challenges in the modelling of physiologically relevant blood vessels is the implementation of circulation inside the model. Although a lot of research on metastasis has been done in a static state, a flow-based experiment gives a better representation of the conditions inside blood vessels. Microfluidic devices designed for this application have gained more interest in the field of biomedical research. A front runner in the field of microfluidic devices is Fluigent with their new organ-on-a-chip platform, OMI [17]. This device has fully automated flow injection and control and can be put inside incubator, making precise, rapid and high-throughput research possible on different subjects of biomedical technology.

With the ability to more and more accurately mimic a physically correct human blood vessel, research on effect of EVs could be conducted with higher reliability. For that reason, the following research question was posed: *Using the OMI microfluidic device, what is the effect of EVs produced by lung tumor clusters on the micro-environment inside both mono-layered and multi-layered VoC models*?

In this study, an optimized VFP method was used for the patterning of both mono- and multi-layered VoCs. To mimic the properties of a blood vessel, mesenchymal stem cells (MSC) were used as the perivascular layer and primary human umbilical vein endothelial cells (HUVEC) for the endothelial layer of the VoCs [18, 19]. To study the effect of EVs, A549 tumor cells were used for producing lung tumor-derived EVs

(tdEVs) [20]. EVs were isolated using common methods for EV isolation [21]. To test the permeability of the formed VoCs, the vessels were filled with either EVs or TNF-α as a positive or plain medium as a negative control for deterioration of integrity. After this experiment, immunostaining for ZO-1 was conducted to analyse the integrity of the vessel barriers [11, 4]. Eventually, a pilot-experiment was conducted to test a flow-based set-up on the channels using Fluigent devices and software. The shear stress was calculated to compare to common high shear stress in capillaries of 40 dyn/cm^2 [22, 23].

2 Materials and Methods

2.1 Microfluidic chip fabrication

Microfluidic chips with straight channels were designed in a 3D CAD software (Solidworks) with the following dimensions: height 0.5 mm × width 0.5 mm and 1.0 cm length for mono-layered VFP and height 1 mm × width 0.5 mm and 1.0 cm length for multi-layered VFP. In- and outlet diameters were set at 1 mm to allow the connection to the tubing of the microfluidic pump. A mold was designed to make 4 chips in one mold. Digital files of the parts were downloaded as SLT file for further use in 3D printing program Formlab. The chip molds were 3D printed using layer thickness of 100 μ and the FL Clear V4 resin with the FORM 3B+. After printing, the molds and especially the channels were rinsed with isopropanol, sonicated for 30 minutes (min) and UV treated at 60° C for 60 min.

Polydimethylsiloxane (PDMS; 1673921, Sylgard 184) and curing agent (761036-5EA, Sylgard 184) were mixed at a 10:1 volume ratio and degassed for 45 min under vacuum at room temperature. The degassed PDMS was then poured over the molds and again degassed for 60 min in vacuum. The PDMS was cured at 65 °C overnight. After curing, the chips were immediately removed from the mold. The PDMS chips were cut from the mold using a scalpel and holes were pre-punched if necessary using a Miltex 1 mm diameter puncher. The PDMS chips were bonded to microscopic glass slides (75 mm × 26 mm × 1 mm) by plasma activation using a quick PDMS binding program on the Femto Science Inc. Covance Plasma Cleaner for 45 seconds with a 30 seconds vent time before contact. As a final treatment, a polydopamine coating was applied to the channels of the chip to allow proper bonding of collagen. A 2 mg/mL solution of polydopamine (PD; H8502, Sigma Life Science) in Tris-HCl buffer (10mM, pH = 8.5) was freshly prepared and the channels were loaded with 10μL of PD solution and incubated for 1 hour (h) at room temperature (RT). After, the channels were washed 3-5 times with 15μL MilliQ water, the chips were put in Petri dishes and dried at 65°C for 1 h. After, the chips were stored at room temperature until use within 3 days.

2.2 Cell culture

RPF-labelled HUVECs (cAP-0001RFR, PeloBiotech) as the endothelial layer and MSCs (PCS-500-012, ATCC) as the perivascular layer were cultured in EGM-2 medium (SCC1001-b, ScienceCell) and alpha-MEM (22571-020, Gibco), respectively, according to the supplier's instructions [24, 25]. HUVECs and MSC were both maintained in T75 tissue culture flasks precoated with 5 mL 1:100 collagen type I-A (sterile, 211012 Cellmatrix) in PBS (D8537, Sigma Life Science) solution for 30 min at 37 C and passaged with a cell density of respectively 10^6 and $0.75*10^6$ cells/mL. All cells were cultured in humidified 95% air/5% CO_2 incubators at 37 C. At a confluence around 90%, the cells were passaged and/or used for the experiment. HUVECs were used between passage (PS) 8 and 11, MSC at PS 6. MSCs were loaded with Green CMFDA (C7025, CellTracker, Invitrogen) according to the supplier's instructions before use, allowing multiplex visualisation with the RFP-labelled HUVECs [26].

2.3 Isolation EVs

2.3.1 A549 tumor clusters

To produce correct tdEVs, lung CTCs, the cells responsible for metastasis to take place, were cultured [8]. A549 (86012804, ECACC) were first cultured in RPMI 1640 medium (21875-043, Gibco) containing 10% FBS, pen/strep and glutamax in T75 tissue culture flasks and maintained in humidified 95% air/5% CO_2 incubators at 37 C.

To form the tumor clusters, microwells in a 12-well plate were used. Microwell 3D-printed molds were prepared and stored in ethanol. After cleaning with ethanol and drying inside the laminar hood, the molds were placed inside a 6 well-plate. A mixture of 3.0 g agarose (sterile, 16500, Invitrogen) and 110 mL PBS was prepared. The mixture was microwaved at 700W for 2 min, until all agarose was dissolved, resulting in a 3 mg/mL solution. After, the agarose was poured on top of the molds, creating a 1.5-2.5 mm thick layer. After centrifuge using the Eppendorf centrifuge 5810 R at 300 g with a slow acceleration and slow deceleration for 2 min at RT, the well plate was sealed with parafilm and stored in the fridge for 20 min at 4 C. After hardening, the agarose microwell disks were removed from the molds using a puncher and put inside a 12 well-plate.

After 3 days the A549 cells were detached from the T-75 flask and seeded on the microwells. 1 mL of cell suspension at $0.5*10^5$, $1*10^5$ or $2*10^5$ cells/mL was added drop-wise onto each agarose microwell evenly across the surface. In order to place the cells inside the microwells, the wells were spinned down at 300 g with a slow acceleration and deceleration for 3 min. 2 mL medium was added at the side of the wells and the clusters were maintained in humidified 95% air/5%

CO_2 incubators at 37 C. After 2, 3, and 6 days of culture, the medium of the cells was replaced and the retrieved tumor-conditioned medium was stored in small test tubes at -20 C.

2.3.2 Ultracentrifugation

Ultracentrifugation was applied to isolate the EVs from the tumor-conditioned medium. First, 14 mL tumor-conditioned medium was defrosted. Then, the mixture was centrifuged in a Beckman Coulter ultracentrifuge at 10 min 300 g, in order to remove live cells, next 10 min at 2000 g, to remove dead cells, 30 min at 10,000 g to remove cell debris, and finally 70 min at 100,000 g, all at 4 C [27]. The small pellet that was created was re-suspended in 1 mL EGM-2 medium. The EVs in medium were stored before usage at 4 C in the fridge.

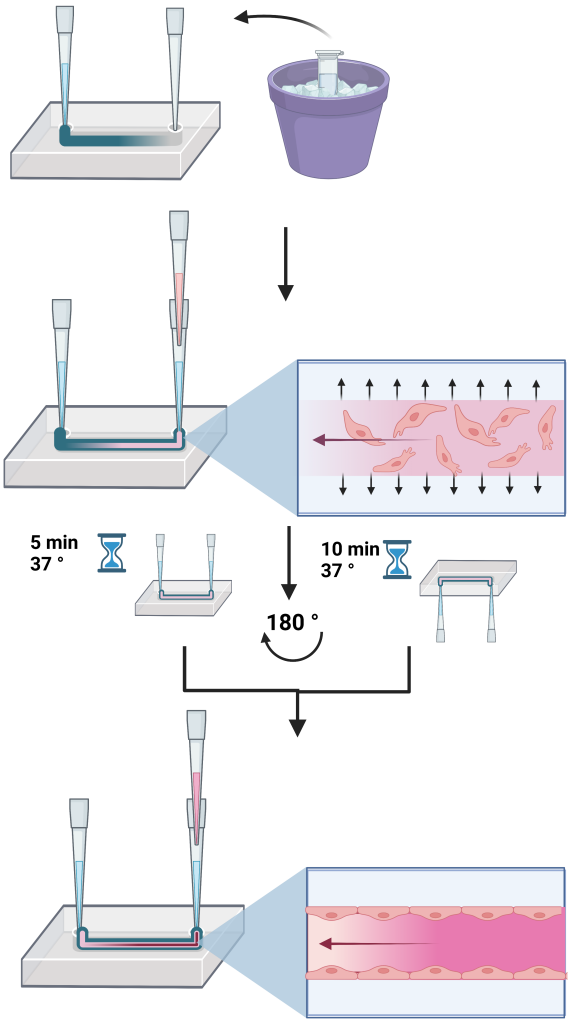

Figure 2: A schematic overview of the process of VFP. Created with BioRender.com.

2.4 VoC model formation by VFP

For conducting the VFP, the micropipettes tips used at the outlets were marked at 7 mm height using a permanent marker [11, 12]. A neutralized collagen solution was prepared on ice by mixing collagen type I-A (sterile, 211012 Cellmatrix) and PBS (Thermo Fisher Scientific) in 1:10 volume ratio. If necessary, a collagen buffer ($NaHCO_3$ 260 mM, HEPES 20 mM, 0.05 N NaOH) was added to a achieve pH value around 7. This was checked using the outlet used pH indicator paper. While working on ice, the channels were filled with 15 μL of collagen solution through one of the inlets until 7 mm mark was reached on the outlet pipette tip. While leaving the pipette tips in place, 7 μL of a HUVEC (10-30*10^6 cells/mL) cell suspensions in 3% dextran medium was injected in the pipette tips inside the outlets. The devices were incubated at 37 C in order to allow collagen gelation and cell adhesion. To ensure the entire surface of the collagen was covered with cells, the chips were flipped 180 after 5 min. An empty micropipette box containing 2 parallel tapes acted as a tool to flip the chip while inside the incubator. The cells were incubated for another 10 min. After the total of 15 min incubation, 15 μL of culture medium was added to the outlet, and the chips were incubated for 24 h. A summary of the procedure is shown in Figure 2. Every 24 h, the medium was changed. To prevent the formation of air bubbles and deterioration of the formed VoCs, the previous pipette tips were first removed in a smooth twisting motion. Using micropipette tip filtered 2-20 μL, one tip was carefully inserted in the outlet and medium was added in the inlet and again the tips were left inside the inlet.

Regarding the multi-layered VoCs: the procedure described above was conducted with a MSC cell suspension (10*10^6 cells/mL) and after 3 h performed a second time with a HUVEC cell suspension (15*10^6 cells/mL) for double VFP, after removing the micropipette tips in a twisting motion.

2.5 Experiment effect EVs of VoCs

After 4 days of culture, a lumen was formed and the VoCs were ready for tests. In order to research the influence of EVs on the VoC integrity, each chip was subjected to different conditions. As a positive control of disruption of VoC integrity, TNF-α (100 ng/mL) in EGM-2-medium and EGM-2 alpha-MEM 1:1 medium mixture for, respectively, mono- and multi-layered VoCs was used [28]. Plain EGM-2-medium and a EGM-2 alpha-MEM 1:1 medium mixture for respectively mono- and multi-layered VoCs were used as a negative control. For the experiment, the EVs in EGM-2-medium and the EVs with added alpha-MEM medium 2:1 were used for, respectively, mono- and multi-layered VoCs. The VoCs were injected with 15 μL of the above mentioned mixtures and incubated for 2-3 h in humidified 95% air/5% CO_2 incubators at 37 C. Later, the channels were fixated as explained in 2.6 Fluorescent Staining and Imaging.

2.5.1 Indication of the presence EVs using EpCAM

In order to indicate the presence of actual lung tumor cluster-derived EVs (tdEVs), a 2D culture of HUVEC cells was prepared. In a 96 well-plate, 16 wells

of HUVEC were prepared and cultured according to a standard protocol. After 3 days of culture, EGM-2-medium, EGM-2-medium containing EVs and TNF-α in medium (100 ng/mL) were respectively added to 6, 6 and 4 wells. After 3h, the cells were fixated as explained below.

2.6 Fluorescent Staining and Imaging

To indicate disruption of endothelial integrity, the staining of the ZO-1 was conducted and analysed. Because of their high expression in lung tdEVs, a staining for the EpCAM protein was used on the 96 well-plate to indicate the presence of EVs [29]. The chips and microwells of all experiments were stained using standard immunostaining procedures. First, channels were washed with 1x PBS at least 3 times. Then, the cells were fixated with 4% paraformaldehyde (PFA; P6148, Sigma Aldrich) at RT for 30 min and again washed 3 times using 1x PBS. After this, the chips and wells were either stored for later staining together with other chips or immediately stained. When staining, a 0.1% Triton X-100 in PBS mixture (T8787, Sigma Life Science) was added for 20 min at RT. A blocking buffer of 1% BSA (A7030, Sigma Aldrich) in 1x PBS was added and the chips and wells incubated 1 h at RT. A primary rabbit antibody against ZO-1 (WI333077, invitrogen) and a mouse antibody anti-EpCAM (14-9326-82, invitrogen) were diluted 1:100 in 1% BSA buffer, added to the chips and wells and incubated at 4°C overnight. The next day, the cells were washed with 1x PBS 3 times. Then, a secondary anti-rabbit antibody conjugated with Alexa Fluor 647 (A27040, invitrogen) 1:200, a goat anti-mouse anti-body with Alexa Fluor 488 (A11034, invitrogen) and a DAPI-staining (62248, Thermo Scientific) 1:400 in 1% BSA buffer was added to the chips and wells and incubated for 1,5 h at RT. For the 96 well-plate, a third stain was used Finally, the chips and wells were washed with 1x PBS at least 3 times. Fluorescence images were acquired by scanning confocal microscopy using the Zeiss LSM880. Images were processed using ZEN lite and ImageJ Java software and 3D reconstruction images were generated using the 3D viewer plugin.

2.7 Pilot experiment: flow-based set-up

When the OMI arrived for experimental use, it appeared to have a lot of bugs. To replace the OMI with another perfusion system, other devices of Fluigent were used, see Figure 3. A set-up was used which pumped medium from one test tube through the channel using 1 mm diameter channeling to another tube. The experiment was controlled and monitored using the Oxygen software by Fluigent. VoCs were subjected to flow ranging from 0 to 1000 um/min to determine when cells would detach from the VoCs. This would then be the maximum flow rate and half the value of this rate was used to subject the chips to for the flow-based experiment. The VoCs were real-time recorded using the Olympus IX51 microscope with a RFP filter and a frame rate of 1 frame per 30s The recordings were later analysed using ImageJ software.

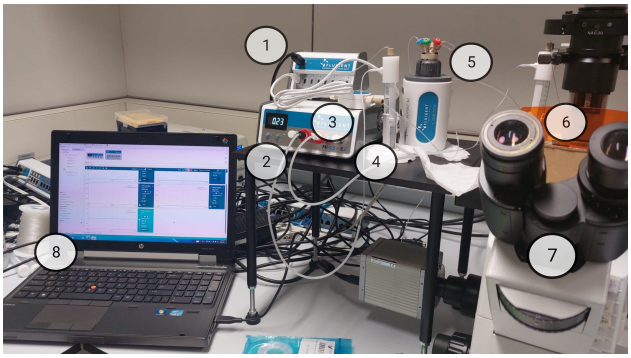

Figure 3: A photo of the flow-based set-up for testing of the chips with (1) flow rate platform (2) pressure controller (3) flow unit (4) test tube filled with EGM-2 medium (5) L-switch (6) empty test tube as a reservoir connected to the experimented chip (7) Olympus IX51 microscope using RFP filter (8) laptop with Oxygen Fluigent software

As an approximation for the density and velocity values of EGM-2 medium, DMEM with around 2% FBS was chosen, giving values of 1.001 g/cm^3 for density and of 0.800 mPa·s dynamic viscosity [30]. Using dimensions of the formed lumen and the viscosity and density of 2% FBS DMEM as EGM-2 medium, the applied shear pressure was calculated using the Darwin Microfluidics shear stress calculator [23].

3 Results

3.1 Microfluidic chip fabrication

Chips with dimensions as mentioned in 2 Materials and Methods were produced, see Figure 4. It is important to mention that the distance between channels was carefully chosen. During practice, the micropipette tips would overlap and hinder each other if the channels were to close together, making the VFP less reproducible for each channel. Thus, I took a distance of 7 mm.
The in- and outlet diameter were set at 1 mm and the connection of the tubes of microfluidic devices was successful.
During production of the chips, sometimes the columns inside the mold used for the chip in- and outlets would break and the in- and outlet had to be manually punched. However, this resulted into poor VFP data. Therefore, it is necessary to use pre-punched chips for VFP experiments.

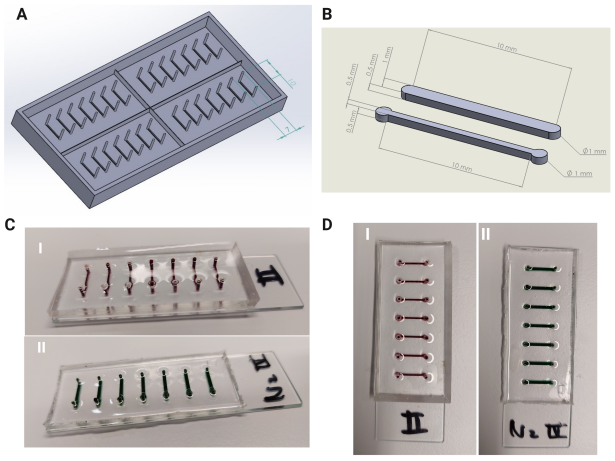

Figure 4: (A) Photo of schematics and dimensions of the microfluidic chip molds in Solidworks (B) Photo of schematics and dimensions of the channels for the mono-layer VFP (bottom) and multi-layer VFP (top) (C) Side-view of microfluidic chip for the mono-layer VFP with red food dye added to the channels (I) and multi-layer VFP with green food dye (II) (D) Top-view of microfluidic chip for the mono-layer VFP with red food dye added to the channels (I) and multi-layer VFP with green food dye (II)

3.2 Cell culture

The HUVECs were cultured from passage 6 up to passage 10, see Figure 5. These cultures showed characteristic adjacent cells and a high confluence and were used for VFP.

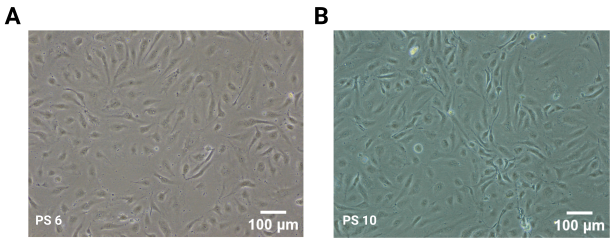

Figure 5: Microscopic photos of (A) HUVECs during PS 6 with a confluence around 80% (B) HUVECs at PS 10 with a confluence around 90%

However, at passage 11, cell behaviour started to deteriorate. The cells would either have a very long stretched morphology or a structure with multiple small extensions, see Figure 6. The cells lost their characteristic closely-packed and moderately-stretched behaviour and the cells would not reach high confluence anymore. These cells were not used for VFP. During the MSCs culture, no abnormalities were noticed.

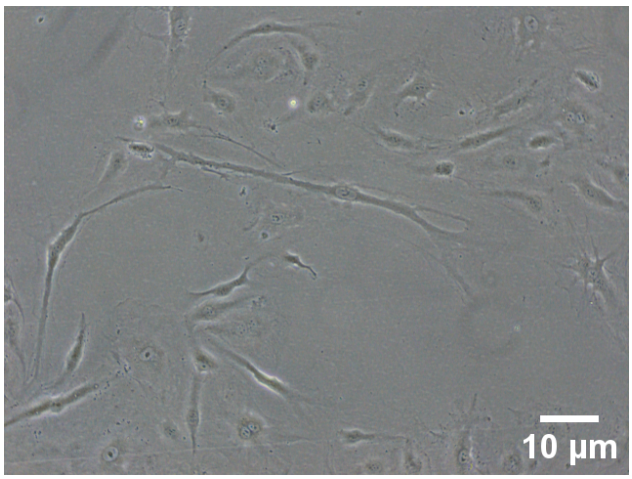

Figure 6: Microscopic photos of deteriorating HUVECs PS 11. Both very long stretched morphology (left) and one with multiple small extensions (right) are visible

3.3 Isolation EVs

3.3.1 A549 culture

A549 cells were cultured and medium was added, see Figure 7. After 2 days, the microwells with a seeding density $0.5*10^5$ cells did not form clusters. However, all tumor-conditioned medium was collected. After 6 days, all microwells contained complete clusters and all the CTC-conditioned medium was collected in one tube and used for experiments on tdEVs.

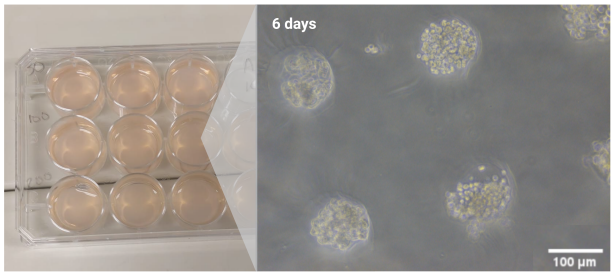

Figure 7: Photo of 12 microwell plate (left) and a close-up of the tumor clusters cultured (right). Small round clusters of A549 cells are visible

3.3.2 Ultracentrifuge

The CTC-conditioned medium was defrosted and ultracentrifuged. During all the steps except for 30 min at 10.000g, a pellet was visible. This could indicate the lack of cell debris inside the medium. After the last step of centrifuge, a small pellet was visible. This pellet was re-suspended in medium and used for the EV experiments.

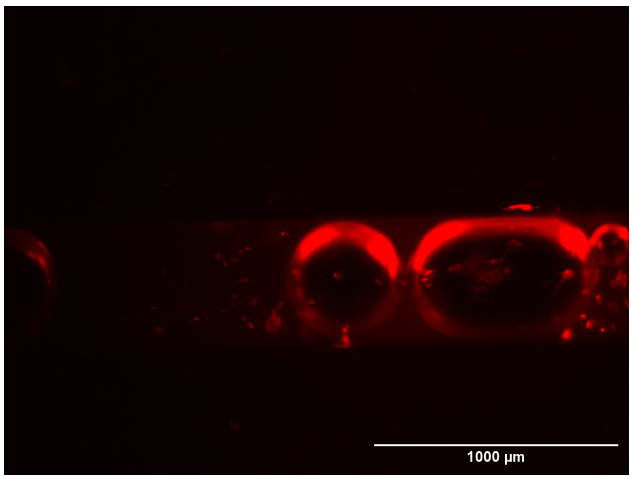

Figure 8: EVOS picture using RFP filter, showing few HUVECs and 3 big air bubbles blocking the chip channel in red

3.4 VoCs by the use of VFP

3.4.1 Mono-layered VoCs

A total of 4 chips with 7 channels each were used for mono-layered VFP. Frequently during the VFP, air bubbles were formed, either during the injection of the collagen, cell suspension or medium. But also, air bubbles were later formed and only noticed the next day after inspection with the life technologies EVOS FL microscope. These air bubbles obstructed the patterning of the complete channel, see Figure 8.

In most cases, even when there were no air bubbles visible, you could notice that the channels were not entirely patterned. At the outlet of the channels, most patterning had taken place. Closer to the inlet, less cells reached the channel, giving a weak RFP signal. However, a total of 5 VoCs were successfully formed. After 4 days of culture, a stronger RFP signal was visible and consistent lumen seemed to be made, see Figure 9.

3.4.2 Multi-layer VoCs

Due to time constraints and material shortage, only 1 chip was used for multi-layered VFP. After 3,5 h, the VFP technique was carefully repeated with HUVECs in order to prevent formation of air bubbles after the patterning with MSCs. After 1 day, a signal for both cell layers seemed to be visible with the EVOS. 4 channels out of 7 had (partly) patterned lumens, as seen in Figure 10. The other 3 contained either too little cells or air bubbles.

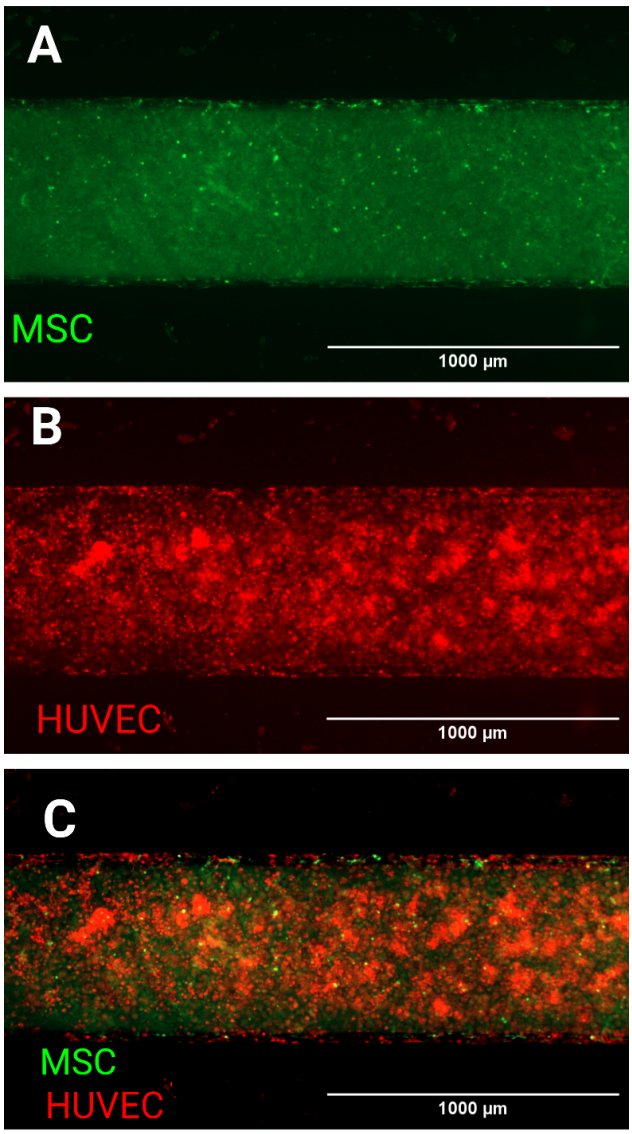

Figure 10: EVOS pictures using (A) RFP filter, showing HUVECs in red (B) GFP filter, showing MSCs in green (C) above filters, showing what seems to be a consistent lumens after 4 days

3.5 Integrity assay of VoCs

3.5.1 Mono-layer VFP

For testing the integrity of the mono-layered VoCs, one chip was subjected to either the control or experimental condition. The chip which consisted of the most patterned lumens was used for the experiments with EVs. If only some parts over the length of the channel were patterned, the best patterned part was analysed.

For the chip containing plain medium, weak signals were visible for HUVECs, see Figure 13. Although the EVOS microscope seemed to show a complete consistent lumen, the confocal microscope showed that only parts of the channel were completely patterned. Especially the top of the chip did not consist of a adherent layer of cells, see Figure. The parts that were patterned, did not show a good lumen, but rather a adhesion of cells in the form of a trapezium, see Figure 13. The square-like form could indicate that no col-

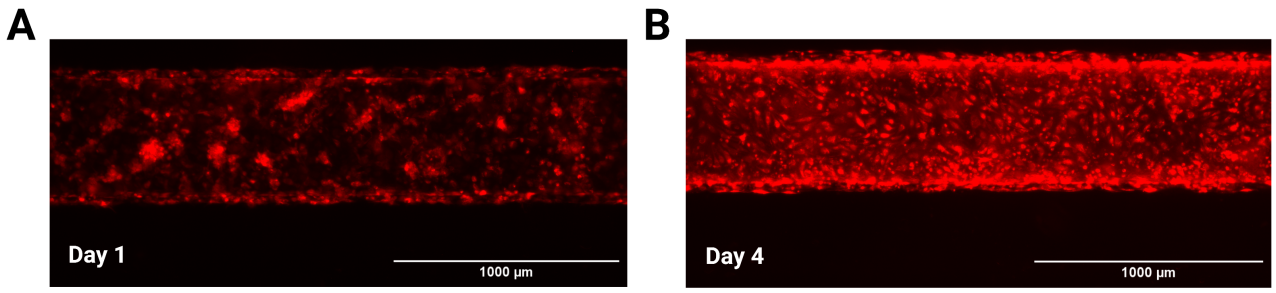

Figure 9: EVOS picture using RFP filter, showing HUVECs in red (A) after 1 day of patterning inside the chip with 60% intensity. HUVECs are visible in lumps through the channel. (B) after 4 days of culture inside the chip with 70% intensity. A lot of HUVEC are visible and seem to form a consistent lumen

lagen layer had been created to which the cells could adhere to to form a good cylindrical lumen. They rather adhered directly to the PDMS and microscopic glass. However, in that case you would expect to see the designed square channels, not a trapezium. To check this, the cross section of the chip channel was inspected11. The designed square outline was visible, ruling out errors during 3D printing. A possible explanation for the trapezium form could be that the corners of the channel did not adhere correctly to the microscopic glass after the plasma treatment, leaving more space for collagen and cells to adhere.

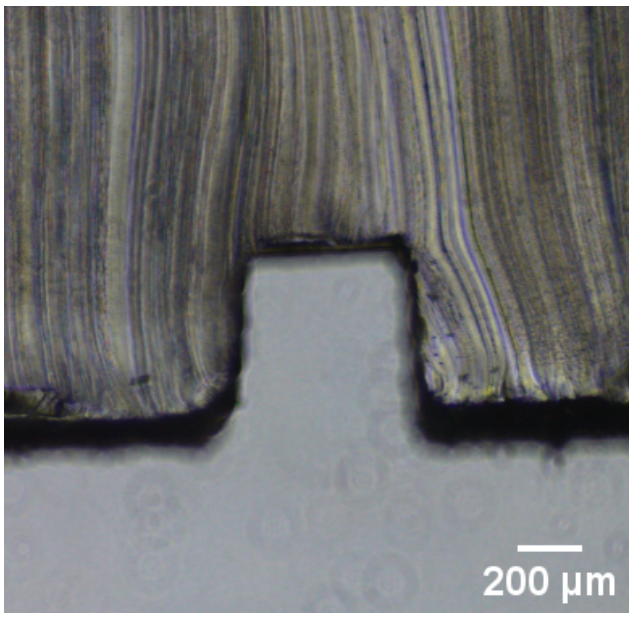

Figure 11: Microscopic picture of cross section of the channel on the used mono-layered microfluidic chips

The VoCs of chips containing the TNF-α and EVs showed with the EVOS a good RFP signal. However, when looking with the confocal microscope, the HUVECs completely lost their RFP signal, see also Figure 12. If there was a RFP signal present, these gave a weird spot-like signal. This deviates from the signal seen on other chips. For this reason, it was not possible to conclude if there was a lumen visible, since only the DAPI staining could give away the structures of the VoC.

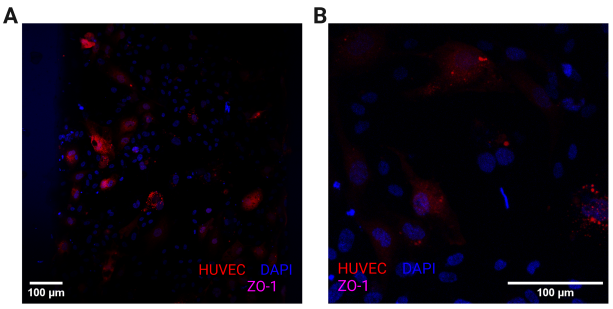

Figure 12: Picture confocal microscope using RFP, DAPI and Alexa Fluor 647 filter, showing (A) mono-layered VoCs (B) a close-up of mono-layered VoCs Both pictures show cell nuclei in blue and an abnormal RFP signal inside the cell cytoplasm

But most remarkable, although parts of some VoCs seemed patterned, no signal for ZO-1 was visible on any of the chips. This indicates that no tight junctions had been formed in any of the VoCs, see Figure 13.

3.5.2 Multi-layer VFP

For testing the integrity of the multi-layered VoCs, 2 channels were exposed to EVs, 2 to plain medium and 3 to TNF-α. The channels with the best patterned lumens were used for the EVs. For partly patterned VoCs, only the best patterned part was analysed.

When analysing with the confocal microscope, it was clear that not all parts of the VoCs were evenly patterned. Some parts were only patterned with HUVECs, other parts only with MSCs. Even VoCs were visible with mainly HUVECs patterning at the outlet or top and MSC patterning at the inlet or bottom. However, one channel seemed to have a real multi-layered VoC, see Figure 14E. When looking at the footage of the channel from top to bottom, first the MSCs would appear followed by the HUVECs. However, when looking closely at the formed layer, not two separate, but rather one mixed layer was visible, see Figure 14F. Also, just like for the mono-layer VoCs, a trapezium was patterned instead of a real lumen, see Figure 14F and G.

Again, just like for the mono-layered VFP, no signal for ZO-1 was visible on any of the channels, indicating no formation of tight junctions, see Figure 14. We

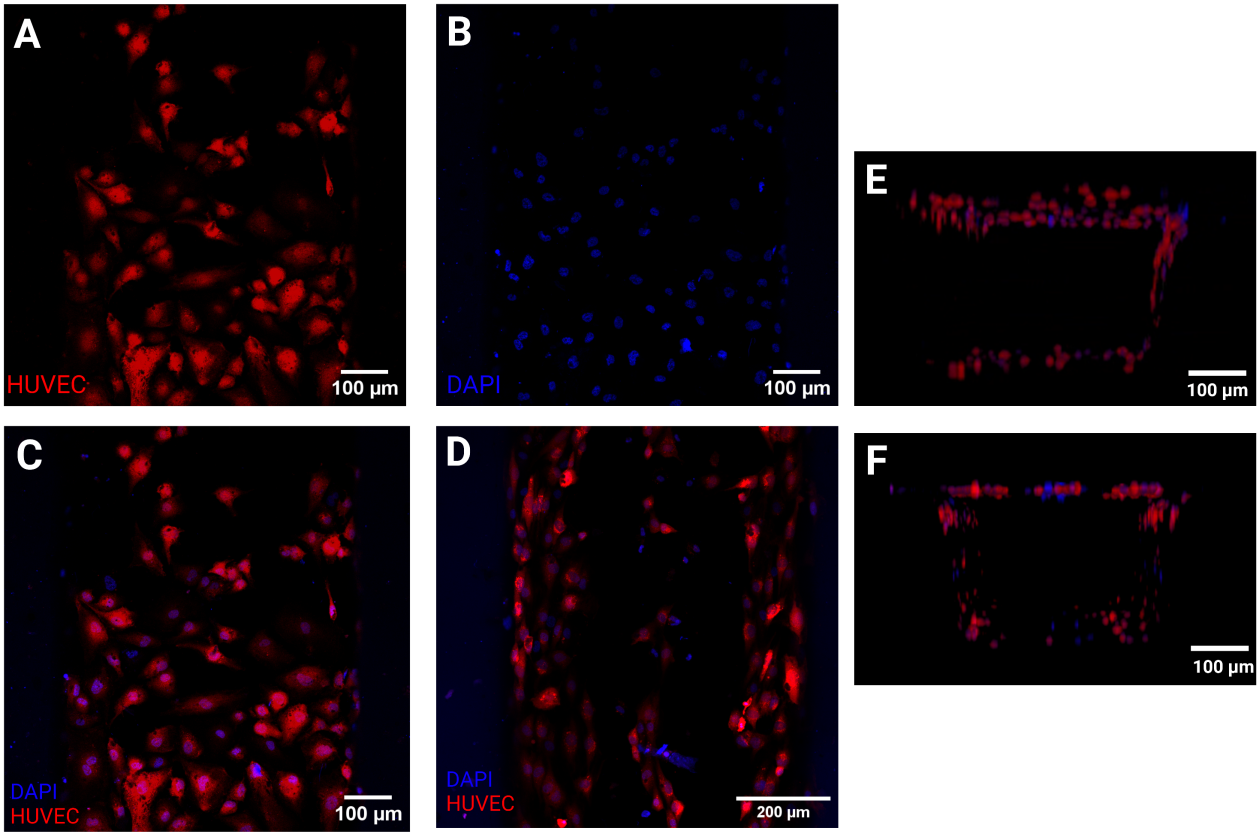

Figure 13: Confocal microscope pictures using (A) RFP filter, showing the HUVECs cytoplasm in red (B) DAPI filter, showing the HUVECs nucleus in blue (C) above mentioned filters, showing the multi-layer VoC. (D) A picture of the channel used for flow-based experiment, showing HUVECs and their nuclei. There is no evident difference between this VoC and the one in (C). (E) A 3D viewer picture of the VoC side-view, showing HUVECs patterned over most sides of the channel in the form of a trapezium. (F) A 3D viewer side-view picture of the VoC used during the flow-based experiment. Again, no evident difference between this VoC and the one in (E) is visible.

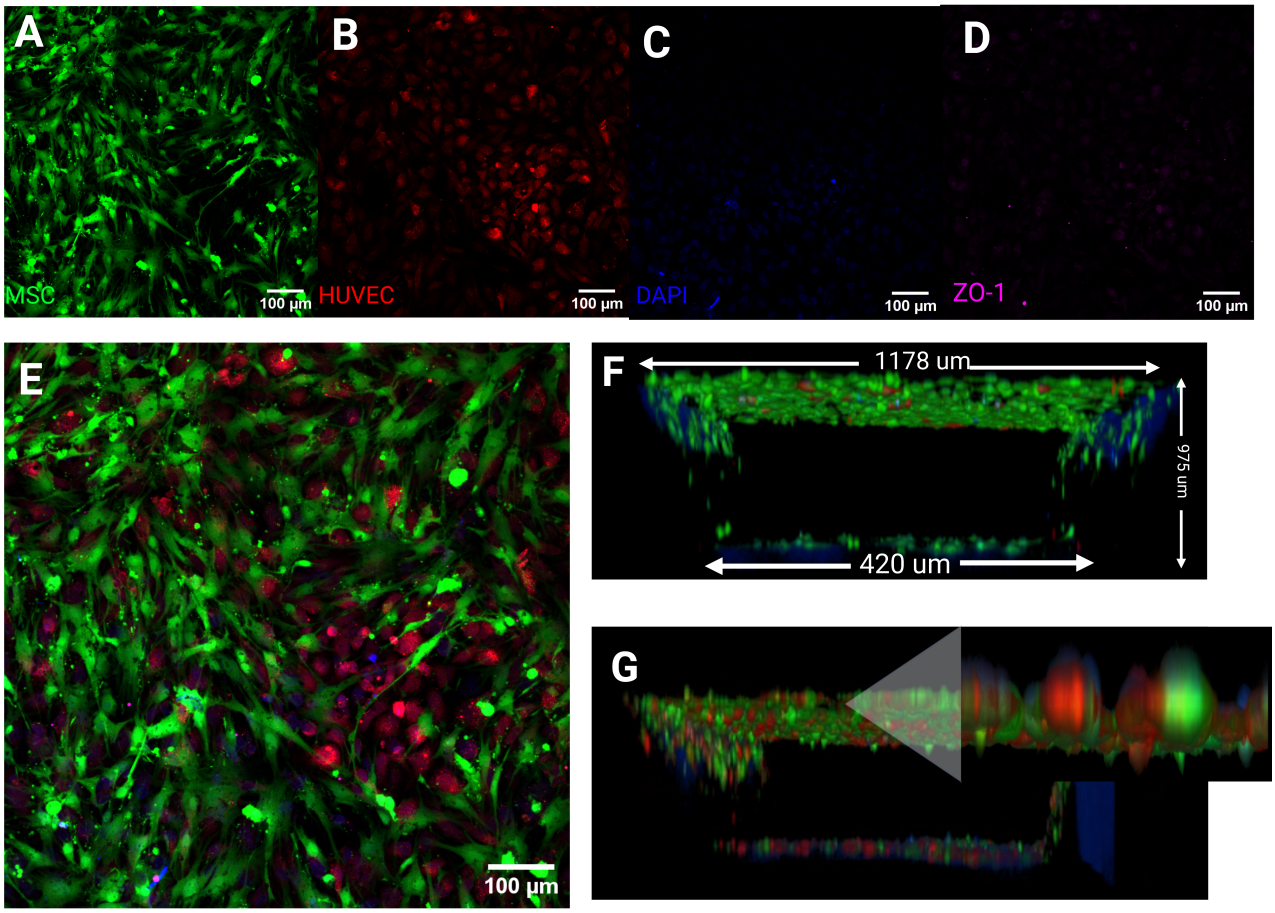

Figure 14: Confocal microscope pictures using (A) GFP filter, showing cytoplasm of the MSCs in green (B) RFP filter, showing the HUVECs cytoplasm in red (C) DAPI filter, showing the HUVECs nucleus in blue (D) Alexa 647 filter, showing the ZO-1 staining in purple (E) above mentioned filters, showing the multi-layer VoC. (F) A 3D viewer picture of the VoC side-view, showing mainly MSCs patterned over the sides of the channel in the form of a trapezium. Dimensions are given width: 420 um height above: 1178 um height below: 975 um. (G) A 3D viewer picture of the VoC side-view, showing both HUVECs and MSCs patterned over the sides of the channel in the form of a trapezium. With a close-up (right), not two separate layers but one mixed layers of red and green is visible.

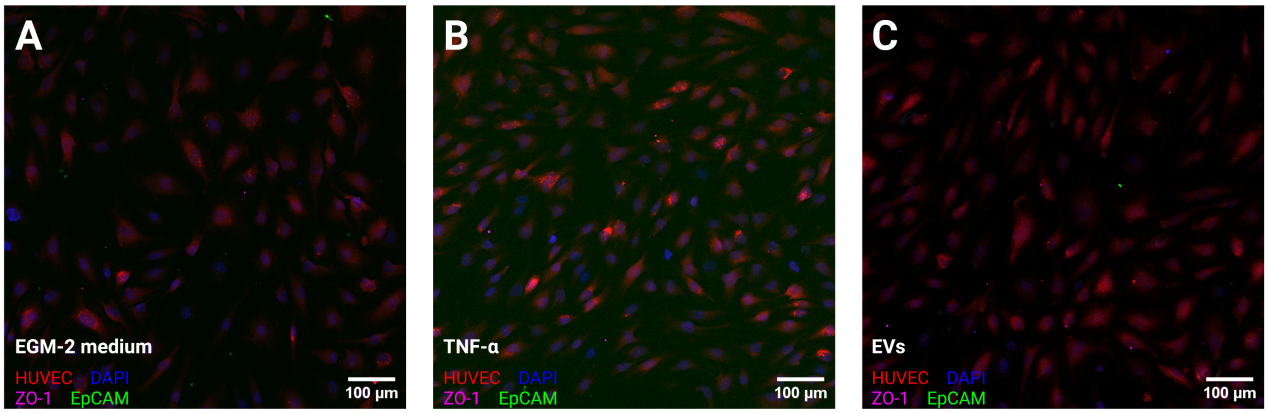

Figure 15: EVOS picture using DAPI, RFP, Alexa Fluor 488 and Alexa Fluor 647 filters, showing the cell nucleus in blue, HUVECs cytoplasm in red, ZO-1 in purple and EpCAM in green for (A) Plain EGM-2 medium (B) TNF-α (C) EVs inside EGM-2 medium. Neither a fluorescent signal from the ZO-1 or EpCAM is visible. Only some small dots where aspecific fluorescence occurs.

even tried re-staining the sample, however this also did not help.

3.6 Indication of the presence of EVs

During the seeding of HUVECs on the 96-well plate, the confluence differed greatly between wells. During culture, some cells were already getting apoptotic, while in other wells the confluence stayed very low and adjacency between cells did not yet seemed to occur. After 4 days, the wells were incubated with the EGM-2 medium, TNF-α and EVs. When analysing using the confocal microscope, no differences were noticeable between the different conditions: only RFP and DAPI signals were visible with sometimes a dot of Alexa 647 or 488 signal, see Figure 15. This probably indicated aspecific fluorescence, not a signal from ZO-1 or Ep-CAM.

3.7 Pilot experiment: flow-based set-up

During set-up, some cells already detached from the formed VoCs. An explanation could be that the pressure applied when inserting the connecting tubes to the in- and outlet 'blew away' the cells. To see when the cells would actually detached because of applied shear stress, a flow from 0 to 1000 uL/min was applied to a partly patterned VoC. At 320 μL/min one cell detached from the patterned HUVECs. However, after increasing the flow up to 1000 μL/min, no cells detached anymore. This could indicate the formation of strongly attached patterning. A flow rate of 400 μL/min was picked for conducting the flow based experiment on the channel with the best formed lumen. The experiment was real-time recorded. During the recording you can see detachment of two cells from the VoCs. Apart from this, no deterioration is visible.

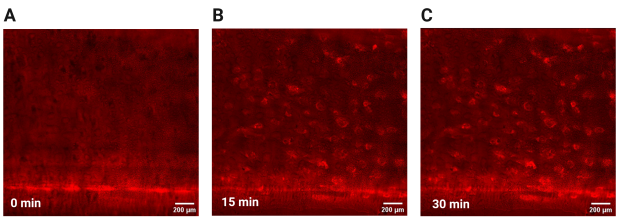

Figure 16: Picture Olympus microscope using RFP filter, edited using ImageJ, showing HUVECs in red in (A) mono-layered VoCs subjected to 400 uL/min flow after 0 min (B) mono-layered VoCs subjected to 400 uL/min flow after 15 min (C) mono-layered VoCs subjected to 400 uL/min flow after 30 min The first picture is out of focus. Picture (B) and (C) show no difference in signal

The applied shear stress was calculated using the Darwin shear stress calculator. This calculator can calculate the shear stress for either rectangular or cylindrical channels. However, in this case, a trapezium lumen was created. To give an estimation of the applied shear stress, the shear stress for both the smaller 420 um x 420 um and 617 um x 617 um bigger square was calculated, see Figure 17. This gave 4,319 dyn/cm^2 and 1,362 dyn/cm^2 respectively, meaning the average shear stress should be around 2,8405 dyn/cm^2. Compared to the shear stress in capillaries of 40 dyn/cm^2 mentioned before in 1 Introduction, this is way lower.

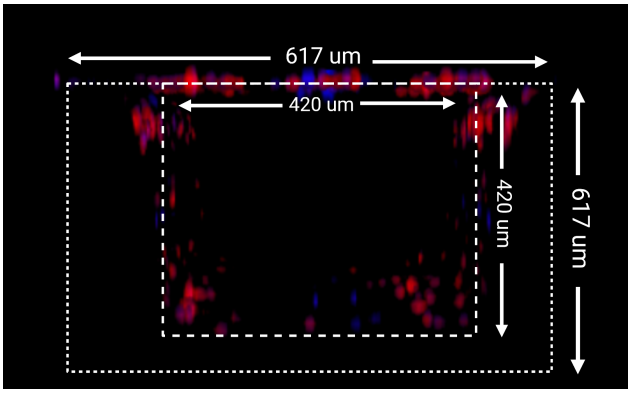

Figure 17: Schematic view of the mono-layer used during flow-based experiment. The big and small square sections used for calculating the shear stress are drawn

The channels were also imaged later using the confocal microscope, see Figure 14. No abnormalities were visible.

4 Discussion

It was very clear that we were not able to form a patterned lumen. As mentioned in the 3 Results, the cells formed a trapezium instead of a cylindrical shape as you would expect from using VFP technique. This probably indicates that rather than a separate layer of collagen with a layer of adhered cells, either one mixed layer with both collagen and cells or no collagen layer at all had been created during VFP. There are multiple explanations for this.
The first would be that the dextran concentration in the cell suspension was too high. This would make the cell suspension so viscous that it completely mixes with the collagen layer, not creating a separate hydrogel layer the cells can adhere to. The second explanation could be the consistency of the used collagen hydrogel. The viscosity of collagen is highly dependent on its concentration [12]. Using hydrogel solutions with a lower concentrations than 6.0 mg/mL Type I collagen often leads to cells invading into the hydrogel rather than forming an intact monolayer lining the hydrogel [31]. Since the collagen solution was $\gg$ 6 mg/mL, incorrect mixing of the collagen could maybe be a reason of failure. In the VFP protocol it is also recommended to use the collagen mixture within 10 minutes. A lot of the VFP was done on the same day and with each chip taking quite long to treat, this was probably not done within the time limit. Another explanation could be the properties of the microfluidic chip. Treatments like plasma treatment can make the surface more hydrophobic, not encouraging the adhe-

sion of hydrogels. To counteract this, the channels are treated with a polydopamine coating. An error during this treatment could explain the lack of adhesion of the collagen hydrogel.

During this study, we did not manage to completely pattern the channels of the chips. Although an explanation could be the lack of collagen as mentioned above, the difficulty of the VFP technique should be emphasized.
Although renowned for its simplicity and reproducibility, a lot of conditions must be met for the VFP technique to succeed. In this study, an already optimized protocol for VFP was employed. In this protocol, the use of micropipette tips is emphasized and should counteract the formation of air-bubbles, which is the major cause of failure of patterning [12]. Also the level the collagen reaches inside micropipette tips determines the hydrostatic pressure responsible for the passive pumping of the cell suspension and thus impacts the consistency of the formed lumens. For this reason the 7 mm marked micropipette tips were used to indicate the desired level of collagen.
Still, a lot of air bubbles were formed, not only in the channels mentioned in the above results. While conducting the VFP, I created a lot of air bubbles either while introducing the collagen inside the channel, injecting the cell suspension or medium inside the outlet. To prevent the first scenario, you could wash the channels with PBS before and after introduction of the collagen. However, in my case it only made it worse. For the other two scenarios, I used reversed pipetting in order to keep a bit of solution and thus all the air inside of the micropipette. This really improved the VFP technique.
However, there were also air bubbles created after VFP, so not due to human factors. A reason for this could be that the created hydro-static pressure was insufficient for the cell suspension to reach the inlet. This could be caused by the drop size of cell suspension: a smaller droplet creates a higher force [12]. The used volume of the droplet was higher than in most protocols (7 μL), so it could be adjusted to for example 5 or 3 μL. Also the size of the inlets is of importance [12]. Although it seemed that for the multi-layered VFP the VoCs were completely patterned, a real multi-layer was not formed, but a mixed one. Again this could be explained by the reasons mentioned above like the invasion of the cells inside the collagen layer.

Also, no tight junction formation was seen in either the 2D (96 well-plate) or 3D (VoCs) culture. This could be because of the use of unhealthy or too old cells, the use of a too low cell density or the use of different media [24].
The use of unhealthy cells can be the main reason of the lack of the formation of tight junctions. As can be seen from Figure 6 and as mentioned in the results, the HUVECs showed very deteriorated behaviour. This very stretched morphology, does not encourage the cells to adhere to each other and thus form tight junctions.
Another explanation could be the lack of barrier inducing factors in the VoCs. To induce the HUVECs to form a proper endothelial layer, structures can be built inside *in vitro* models or flow can be applied to encourage the formation tight junctions [32].

Something else worth mentioning regarding the HUVECs is the lack of RFP labelling. This behaviour only occurred in the chips with the EVs and TNF-α. However this was probably caused by imaging conditions, since in the 2D culture, the RFP signal was still visible for both EVs and TNF-α conditions. Since the supplier of the HUVECs does not say what protein is exactly labelled, it is really hard to explain this behaviour. Because of this lack of signals and thus data, no conclusion can be made on the influence of EVs and TNF-α on the created VoCs.

Whether or not there were actually tdEVs obtained during the experiments, is debatable. After ultracentrifugation only EVs should be left and since a pellet was visible, this probably would have contained tdEVs. However, no signal of EpCAM was visible after staining. An explanation could be that the EVs are more difficult to stain because of their properties: they are nanosized and have physiochemical properties that could influence the staining [33].
Also further research on EVs shows that the isolation and detection seems more challenging than assessed [14, 16]. Another probability is that no tdEVs were actually left on the 2D culture after removal of the medium and the washing step during the staining process. If there would have been a signal visible, the presence of EVs could still be debated. Although EpCAM is used as membrane marker of cancer cells, it is not a specific marker for EVs, [29]. This signal could also have originated from other sources than the EVs.

Also there is still the question left if the correct tdEVs were used.
In this study, a mixture of CTC-conditioned medium for different cell seeding density for different days was used. Because of this, we don not exactly know how much EVs we actually obtained and what kind of EVs. Since EVs have specific integrins that are responsible for the PMN formation, it is important that the correct tdEVs are obtained and used to see an effect [4]. Also the concentration needs to be the same as in the blood of cancer patients to properly mimic the role of tdEVs in organ intercommunication and thus PMN formation [4].

As mentioned in 1 Introduction, it is important to mimic the properties of blood vessels for reliability of research. Flow is really important for the behaviour of the endothelial layer inside blood vessels [22]. Thus, to actually see the effect of EVs, all VoCs should be subjected to flow. The shear stress applied during the

flow-based experiments was way lower than in *in vivo* experienced stress inside blood vessels. This was because the used flow rate was based on a trial-and-error with a limited maximal flow of the Fluigent flow unit. Also the exact applied shear-stress could only be determined afterwards, since the diameter and other properties of the vessel were only visible afters staining using the confocal microscope.
The general outcome of the conducted flow experiment can also be questioned. Apart from using a cumbersome method of calculating the applied shear stress, the conditions did not lend for a reliable flow-based experiment. When vessels are not perfectly cylindrical, they can lead to inconsistencies during flow-related experiments [11]. However the VoCs experimented were rectangular, not consistently patterned channels, giving a worse distribution of shear-stress forces and distorted results.
Apart from this, the experiment were conducted outside of a sterile incubator. This made the conditions very toxic, which could have influenced the behaviour of the cells and outcome of the experiment.

Lastly, during this study, only parts of VoCs were analysed after imaging. Also the amount of experiments is very low because of the high rate of failure, about n= 10. The data obtained thus can not be representative and are inconclusive.

In conclusion, because of the lack of a properly formed endothelial layer with mono- and multi-layered VFP and thus incorrect patterning inside the chip, no conclusion can be made on the conducted experiments on the VoCs. The VFP method is not as easy and reproducible as research before has showed. Since the presence of EVs could not be indicated, the effect of these on the VoCs could also not be studied. We were able to create VoCs which could endure shear stress up to 2,8405 dyn/cm^2, however this did not meet the real-life flow conditions in capillaries.

5 Future Research

5.1 Future Experiments

In future research, I recommended to first study factors that influence the VFP technique specifically for the designed chip in order to optimise the protocol. The main focus should be the adhesion of collagen before the seeding of the cells inside the channels. You could do this by adding a incubation step of collagen and PBS or medium before cell seeding [34]. To ensure the complete patterning of the VoC, a continuous rotary device could be used, provided that can be stalled inside an incubator. You could also try out other techniques using several seeding steps with 90 rotations [10, 35]. However, these are less efficient and more time consuming than the VFP. You could also utilize microfluidic devices during different steps of the VFP to help create continuous and evenly lumens [36]. This way, a more controlled flow can be applied to the used fluids and no human factors can play a role.

Also another batch of HUVECs that does not deteriorate as quick and shows characteristic endothelial behaviour should be used for patterning of the VoCs. If you want to better mimic properties of the perivascular layer, I recommend also to replace MSCs with cells like Normal human lung fibroblasts (NHLF). These cells were previously shown to behave as perivascular cells *in vitro* [11].

To ensure the use of real correct tdEVs in next experiments, a EVs characterisation needs to take place in future research. This can be done by nanoparticle tracking analysis (NTA), scanning electron microscopy (SEM) imaging, and western blot with various protein markers [13]. Isolation of the EVs can also be done by novel techniques using microfluidic lab-on-a-chips to prevent the drawbacks of ultracentrifugation [16, 14].

Regarding the design of the microfluidic chip, shorter channels could be used for the current model. It is not necessary to make long channels for simple straight-channel research and it could prevent the formation of air bubbles over the length of the channel. Also, it would be very interesting to mimic more characteristics of blood vessels. For example, by parallel VFP, you could make branching structures and mimic a capillary bed [10]. You can do this by either using one central in- and outlet for all channels [10] or separate in- and outlets and joined connecting channels [9]. Parallel channels would also facilitate conducting microfluidic experiments, since you can test multiple channels in one go instead of one at a time.

Finally, for the flow-based set-up, Fluigent OMI should be used. This way fully automated and continuous circulation can be conducted on the channels inside the incubator. To make sure that VoCs are optimized before these experiments, as mentioned in 4 Discussion, I would recommend using non-destructive analysis of VoCs by checking protein expression using qPCR. This way you can incubate the channels as long as is required and a individual assay can be conducted [11].

5.2 Potential of EVs

In this study, a very simple model of a blood vessel was used to research the effect of EVs for vascular leakage. However, it would be very interesting to also conduct research on other aspects of PMN formation influenced by EVs using more complex models. Multi-organ on a chip(multi-OoC) using a microvasculature could give really interesting insights on interactions between the blood circulation, the primary tumor site and metastatic site [9]. This way, the whole process of preparing of PMN can be researched cancer metastasis can be predicted [9].

Also, finding a way to mimic parts of the immune sys-

tem inside these chips would be very ground-breaking for research in other mechanisms underlying cancer. Especially neutrophils since they emerge as one of the most important immune cells that could control the metastatic process in lung [4]. Also in the field of targeted drug delivery, EVs are on the rise. EVs have high stability and can simultaneously carry biological macromolecules and chemical compounds [6]. Using above mentioned multi-OoC, cancer treatments enabling EVs could be tested.

Although there there are still a lot of challenges to overcome, EVs have great potential for the intervention of lung PMN as a target or carrier for preventing metastasis and treating metastatic tumors. [16, 6].

6 Acknowledgements

I want to thank the Applied Microfluidics for BioEngineering Research (AMBER) for giving me this opportunity to conduct really interesting research on the topic of cancer for my bachelor assignment. I want to thank my head of committee, prof.dr.ir. Séverine Le Gac for all her supervision and feedback and I want to thank my external committee member prof.dr.ir. Nienke Bosschaart for her help and different perspectives on the researched topic.
I want to specially thank my daily supervisor dr.ir. Kirsten Pondman for all her support during my research. Without her help, this research could not be made possible.
I also want to thank Utku Devamoglu as my 'stand-in daily supervisor' for all his help on the lab and during troubleshooting. I also thank Marlowe Noll for conducting the flow-based experiments together. I want to thank all the other students at AMBER for being so kind and helpful during my stay.
And last but not least I want to thank my friends and family for their support after long and challenging days on the lab.

References

1. Longkanker Nederland. Longkanker. 2022 :5641
2. World Health Organisation. Cancer. 2022 Feb. Available from: https://www.who.int/news-room/fact-sheets/detail/cancer
3. Langley RR and Fidler IJ. The seed and soil hypothesis revisited-The role of tumor-stroma interactions in metastasis to different organs. International Journal of Cancer 2011 Jun; 128:2527–35. DOI: 10.1002/IJC.26031
4. Pontis F et al. The metastatic niche formation: focus on extracellular vesicle-mediated dialogue between lung cancer cells and the microenvironment. Frontiers in Oncology 2023; 13:1–13. DOI: 10.3389/fonc.2023.1116783
5. Saviana M et al. Extracellular vesicles in lung cancer metastasis and their clinical applications. Cancers 2021; 13:1–29. DOI: 10.3390/cancers13225633
6. Liu Y et al. Formation of pre-metastatic niches induced by tumor extracellular vesicles in lung metastasis. Pharmacological Research 2023; 188:106669. DOI: 10.1016/j.phrs.2023.106669
7. Kim J et al. Three-dimensional human liver-chip emulating premetastatic niche formation by breast cancer-derived extracellular vesicles. ACS Nano 2020; 14:14971–88. DOI: 10.1021/acsnano.0c04778
8. Kong J et al. A novel microfluidic model can mimic organ-specific metastasis of circulating tumor cells. Oncotarget 2016; 7:78421–32. DOI: 10.18632/oncotarget.9382
9. Picollet-D'hahan N et al. Multiorgan-on-a-Chip: A Systemic Approach To Model and Decipher Inter-Organ Communication. Trends in Biotechnology 2021; 39:788–810. DOI: 10.1016/j.tibtech.2020.11.014
10. Bischel LL, Lee SH, and Beebe DJ. A Practical method for patterning lumens through ECM hydrogels via viscous finger patterning. Journal of Laboratory Automation 2012; 17:96–103. DOI: 10.1177/2211068211426694
11. Delannoy E et al. Multi-Layered Human Blood Vessels-on-Chip Design Using Double Viscous Finger Patterning. Biomedicines 2022; 10. DOI: 10.3390/biomedicines10040797
12. De Graaf MN et al. Scalable microphysiological system to model three-dimensional blood vessels. APL Bioengineering 2019; 3:1–11. DOI: 10.1063/1.5090986
13. Kim J et al. Prediction of tumor metastasis via extracellular vesicles-treated platelet adhesion on a blood vessel chip. Lab on a Chip 2022; 22:2726–40. DOI: 10.1039/d2lc00364c
14. Chiriacò MS et al. Lab-on-chip for exosomes and microvesicles detection and characterization. Sensors (Switzerland) 2018; 18. DOI: 10.3390/s18103175
15. Guo SC, Tao SC, and Dawn H. Microfluidics-based on-a-chip systems for isolating and analysing extracellular vesicles. Journal of Extracellular Vesicles 2018; 7. DOI: 10.1080/20013078.2018.1508271
16. Piffoux M et al. Potential of on-chip analysis and engineering techniques for extracellular vesicle bioproduction for therapeutics. View 2022; 3:1–15. DOI: 10.1002/VIW.20200175
17. Fluigent. Fluigent's new organ-on-chip platform, Omi - Fluigent. 2023 Mar. Available from: https://www.fluigent.com/company/news/fluigent-omi/
18. Medina Leyte DJ et al. applied sciences Use of Human Umbilical Vein Endothelial Cells (HUVEC) as a Model to Study Cardiovascular Disease : Appl. Sci. 2020
19. Pittenger MF et al. Mesenchymal stem cell perspective: cell biology to clinical progress. npj Regenerative Medicine 2019; 4. DOI: 10.1038/s41536-019-0083-6
20. Qi L et al. In vivo Tumor Growth and Spontaneous Metastasis Assays Using A549 Lung Cancer Cells. Bio-Protocol 2020; 10:1–8. DOI: 10.21769/bioprotoc.3579

21. Szatanek R et al. Isolation of extracellular vesicles: Determining the correct approach (review). International Journal of Molecular Medicine 2015; 36:11–7. DOI: 10.3892/ijmm.2015.2194

22. Rocher V. Microfluidic Flow Rate and Shear Stress Calculator– Darwin Microfluidics. 2017. Available from: https://darwin-microfluidics.com/blogs/tools/microfluidic-flowrate-and-shear-stress-calculator

23. McMillan A. Shear stress in microfluidic devices– Darwin Microfluidics. 2017. Available from: https://darwin-microfluidics.com/blogs/reviews/shear-stress-in-microfluidic-devices

24. Cc CN. Human Umbilical Vein Endothelial Cells. Encyclopedia of Cancer 2011 :1760–0. DOI: 10.1007/978-3-642-16483-5{_}2861

25. Merck. Mesenchymal Stem Cell Culture Protocols. Available from: https://www.sigmaaldrich.com/NL/en/technical-documents/protocol/cell-culture-and-cell-culture-analysis/stem-cell-culture/mesenchymal-stem-cell-culture-protocols

26. Bodipy G et al. Quick Reference CellTracker ™ Fluorescent Probes :0–1

27. Théry C et al. Isolation and Characterization of Exosomes from Cell Culture Supernatants and Biological Fluids. Current Protocols in Cell Biology 2006; 30:0–29. DOI: 10.1002/0471143030.cb0322s30

28. Zhou P et al. Attenuation of TNF-α-induced inflammatory injury in endothelial cells by ginsenoside Rb1 via inhibiting NF-κB, JNK and p38 signaling pathways. Frontiers in Pharmacology 2017; 8:1–13. DOI: 10.3389/fphar.2017.00464

29. Malyla V et al. Extracellular Vesicles Released from Cancer Cells Promote Tumorigenesis by Inducing Epithelial to Mesenchymal Transition via β-Catenin Signaling. International Journal of Molecular Sciences 2023; 24. DOI: 10.3390/ijms24043500

30. Poon C. Measuring the density and viscosity of culture media for optimized computational fluid dynamics analysis of in vitro devices. Journal of the Mechanical Behavior of Biomedical Materials 2022; 126. DOI: 10.1016/j.jmbbm.2021.105024

31. Bischel LL et al. Tubeless microfluidic angiogenesis assay with three-dimensional endothelial-lined microvessels. Biomaterials 2013; 34:1471–7. DOI: 10.1016/j.biomaterials.2012.11.005

32. Aman J et al. Using cultured endothelial cells to study endothelial barrier dysfunction: Challenges and opportunities. American Journal of Physiology - Lung Cellular and Molecular Physiology 2016; 311:453–66. DOI: 10.1152/ajplung.00393.2015

33. Biotum. Extracellular Vesicle Labeling - Biotium. Available from: https://biotium.com/technology/exosome-ev-labeling/

34. Bulut M et al. Three-Dimensional Vessels-on-a-Chip Based on hiPSC-derived Vascular Endothelial and Smooth Muscle Cells. Current Protocols 2022; 2. DOI: 10.1002/cpz1.564

35. Tu TY et al. A Facile Method for Generating a Smooth and Tubular Vessel Lumen Using a Viscous Fingering Pattern in a Microfluidic Device. Frontiers in Bioengineering and Biotechnology 2022; 10:1–13. DOI: 10.3389/fbioe.2022.877480

36. Chrobak KM, Potter DR, and Tien J. Formation of perfused, functional microvascular tubes in vitro. Microvascular Research 2006 May; 71:185–96. DOI: 10.1016/J.MVR.2006.02.005